

D13-2004-101

A. S. Artiomov¹, Yu. S. Anisimov¹, S. V. Afanasiev¹,
S. N. Bazilev¹, L. S. Zolin¹, I. B. Issinsky¹, J. Kliman^{1, 2},
A. I. Malakhov¹, V. Matoušek², M. Morháč^{1, 2},
V. A. Nikitina¹, A. S. Nikiforov¹, P. V. Nomokonov¹,
A. V. Pilyar¹, I. Turzo²

CONTROL OF THE BEAM-INTERNAL TARGET
INTERACTION AT THE NUCLOTRON
BY MEANS OF LIGHT RADIATION

Submitted to «Nuclear Instruments and Methods A»

¹Joint Institute for Nuclear Research, Dubna, Russia

²Institute of Physics, Slovak Academy of Sciences, Bratislava, Slovakia

Артемов А. С. и др.

D13-2004-101

Контроль взаимодействия пучка с внутренними мишенями на нуклотроне по световому излучению

На нуклотроне для оперативного контроля и временной оптимизации интенсивности взаимодействия пучка с различными внутренними мишенями можно использовать их световое излучение. Приведены примеры получаемой информации о пространственных характеристиках циркулирующего пучка за один цикл работы ускорителя на стадиях инжекции, ускорения и проведения физических экспериментов.

Работа выполнена в Лаборатории высоких энергий им. В. И. Векслера и А. М. Балдина ОИЯИ.

Препринт Объединенного института ядерных исследований. Дубна, 2004

Перевод авторов

Artiomov A. S. et al.

D13-2004-101

Control of the Beam-Internal Target Interaction at the Nuclotron by Means of Light Radiation

The light radiation from various internal targets at the Nuclotron can be utilized for the operative control and time optimization of the interaction intensity of the beam. The examples presented in the paper illustrate the information about space characteristics of the circulating beam during one cycle of the accelerator run at the stages of injection, acceleration and during the physical experiments.

The investigation has been performed at the Veksler and Baldin Laboratory of High Energies, JINR.

Preprint of the Joint Institute for Nuclear Research. Dubna, 2004

INTRODUCTION

In cyclic accelerators the internal targets are widely used for the purposes of diagnostics of space-time characteristics [1–7] and polarization [8–10] of circulating beam, improving its parameters [11, 12], ion extraction (e. g. by means of bend crystals) [13, 14], forming the secondary particle beams [15], solving tasks by means of target beam crossing the interaction region under predefined angles [16, 17], and for realization of various experiments in physics [18, 19] as well. In particular, the use of this technique at the superconducting accelerator — Nuclotron [20] (Veksler and Baldin Laboratory of High Energies, JINR, Dubna) — gives supplementary possibilities in carrying out investigations in intermediate field of relativistic nuclear physics with beam energy from hundreds MeV to several GeV per nucleon [21]. At the same time one can investigate a gradual transition of the nuclear matter characteristics from proton–neutron to quark–gluon states within unified experimental framework.

The internal target station, which is being used now at the Nuclotron, its potentialities and obtained results are described in [22–28]. For optimization of these investigations the operative control of the interaction intensity of the circulating beam with the targets is based on and realized through the use of light radiation technique. In this work we present the principal results obtained in the experimental investigations carried out in this direction.

LIGHT RADIATION OF THE INTERNAL TARGETS AND THEIR INTERACTION WITH THE BEAM

For the control of the interaction intensity with the target the various secondary particles can be used. The investigations carried out at the Nuclotron, with the number of deuterons $\sim (10^8 \div 10^{10})$ per cycle have proved that for this purpose the photon radiation of the target material in the broad energy range $0,005 \div 3,5 \text{ GeV} \cdot \text{nucleon}^{-1}$ is well suitable. In the experiments we have used the $(\text{CH}_2)_n$, Cu, Al and Au foil targets of dimensions $\sim 4 \times 8 \text{ mm}^2$ and carbon, copper, tungsten and other fibre targets of diameter $8 \div 10 \mu\text{m}$. The foil targets are hung up by on quartz fibres of diameter $9 \mu\text{m}$ in the C-shaped frames, which are attached in vertical position to the holder that is rotated by means of a step motor. To provide the constant stretch of these targets the fibres are connected to the frames through the flat springs of special form. The radiation is detected through the window by a photomultiplier tube and by microchannel-plate detector placed in vacuum. The internal target control system and acquisition of the data from detectors are described in detail in [22, 25]. For chosen foils the experiments have shown that the intensity of light radiation reaches its maximum for thickness of the order of μm or less. In this case practically all mass of the target with

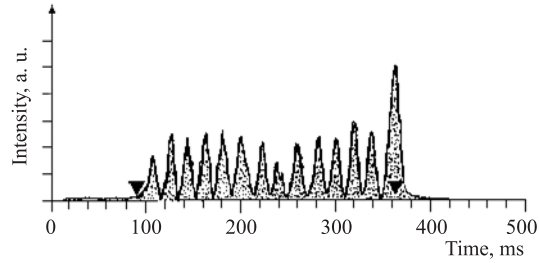


Fig. 1. Time structure of the interaction of a gold foil target of thickness $1.7 \mu\text{m}$ with the circulating deuteron beam at momentum of $3.8 \text{ GeV}/c$. The target light radiation is detected

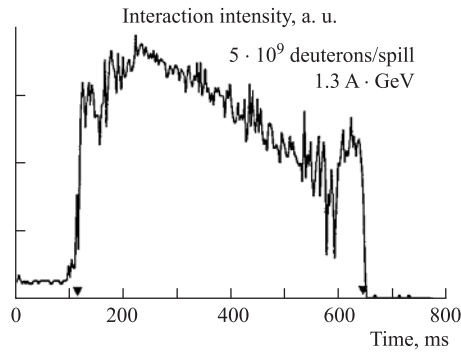


Fig. 2. Time structure of light radiation of a polyethylene target of thickness $1.6 \mu\text{m}$ in its interaction with circulating deuteron beam at energy of $1.3 \text{ A} \cdot \text{GeV}$

high coherent index takes part in its generation. When increasing the thickness of the target this condition is affected and as a consequence at the constant luminosity, averaged over the accelerator cycle run, one can observe a decrease of light radiation. In principle, as a result of the decrease of luminosity the same effect can be observed when changing the target for a heavier one of approximately the same geometrical thickness. In what follows we introduce several examples of data measured in these experiments.

In Fig. 1 we present time dependence of a structure of the light radiation of the gold foil target of thickness $1.7 \mu\text{m}$ interacting with the beam of relativistic deuterons with a momentum of $3.8 \text{ GeV}/c$. The sampling interval was 1 ms . A strong low-frequency modulation of the light signal is caused mainly by a small lifetime ($\approx 2 \cdot 10^{-4} \text{ s}$) of a part of the beam interacting with the target. The same effect was also observed in the experiments with the copper and tungsten fibres. The modulation is practically missing when using CH_2 -target (Fig.2). above

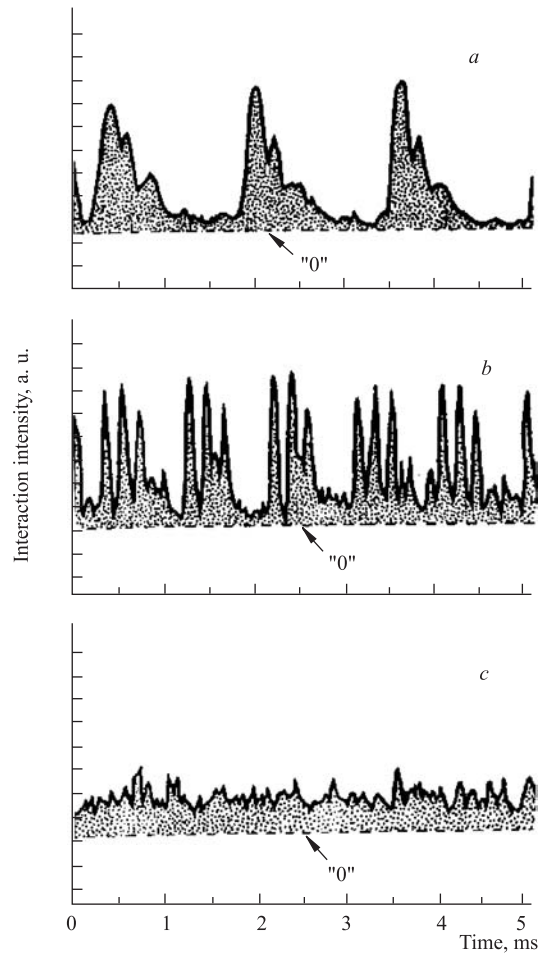


Fig. 3. Microstructure of the deuteron beam interaction with CH_2 -target of thickness $1.6 \mu\text{m}$ at energy of 1.3 GeV/nucleon at various stages of the Nuclotron run: *a*) start of acceleration; *b*) starting point of the "plateau" of the magnetic field; *c*) circulation of the accelerated beam at the switching off the RF-field (disappearance of bunches). The target light radiation is detected

mentioned one. It illustrates the structure and time dependence of the interaction of the circulating beam with targets. In series of carried out experiments the ultraviolet and X -radiation from the targets were detected as well. One can observe a good correspondence among the shapes of the measured signals. A time dependence of the microstructure of the light radiation signals, with sampling

interval 20 ns, is shown in Fig. 3. It corresponds to interaction of the internal target with individual bunches of a beam at the different modes of Nuclotron run.

In [22] it has been illustrated that changing from time to spatial representation of the radiation intensity signal gives the operator a possibility to control the space characteristics of the circulating beam directly during physics experiment. In order to obtain the actual information about the beam profile, the value of a constant speed (V_r) of the thread-like target, crossing the beam, must provide for a sufficiently intensive radiation at the minimum beam perturbation. When having small current of circulating beam and sufficiently large target thickness (in $\text{g}\cdot\text{cm}^{-2}$) the fulfilment of this condition in one cycle of the target motion does not seem realistic. For all that the representation about the beam characteristics can be obtained during its absorption from the side of intersecting target (maximum luminosity mode). At the same time a space-time trajectory of the target motion should be chosen so that the average lifetime of the ions interacting with the target was lower than or nearly equal to the period of discrete thread-like target steps or to time displacement of the foil corresponding to the space resolution. For the orientation the most rapid trajectory ensuring the best space resolution (determined by step of the motor) can be chosen automatically using one operator command. The signals of circulating current (I) and intensity of the foil light radiation (N_γ), which are typical for this kind of experiments, depending on its space position relatively to the beam axis (O_b) are presented in Fig. 4. As mentioned above the observed structure is caused by discrete steps of the target in the space-homogeneous beam. To a considerable extent it is more apparent for the targets with shorter lifetime of the beam. The attachment of the trajectory to the boundary of a beam transfer line (A) in the interaction region allows one to determine the half-width (R_{bx}) and a horizontal position of the beam according to the axis (O). For characteristics of the foil and beam presented in Fig. 4 and for the time of interaction ≈ 0.3 s the attainable resolution in the space of the target motion is estimated to ≈ 0.3 mm. In series of physics experiments with the thin carbon fibres we have used N-shaped target (Fig. 5). It allowed carrying out the acquisition of the events together with the operational control of the beam (B) space characteristics in both horizontal (X) and vertical (Z) directions [29]. In the lower part of figure we present the typical form of the detector signal of the light radiation depending on time. The known distance L_c between the vertical fibres 1 and 3 provides one with the scale that can be utilized for determination of the horizontal beam profile independently of the speed of target motion. Changing the speed influences only the scale of the time axis (t) and the correlation of the light intensities of the fibre 1, 2 and 3, respectively. The value of the horizontal beam size achieved from these measurements is in good agreement with the results obtained from the foil targets or individual fibres used in the same Nuclotron run. Actually for experiments with deuteron energy of 1.6 GeV/nucleon this value was $2R_{bx} \approx 4$ mm at half-height of the beam distribution (see also Fig. 4). When the

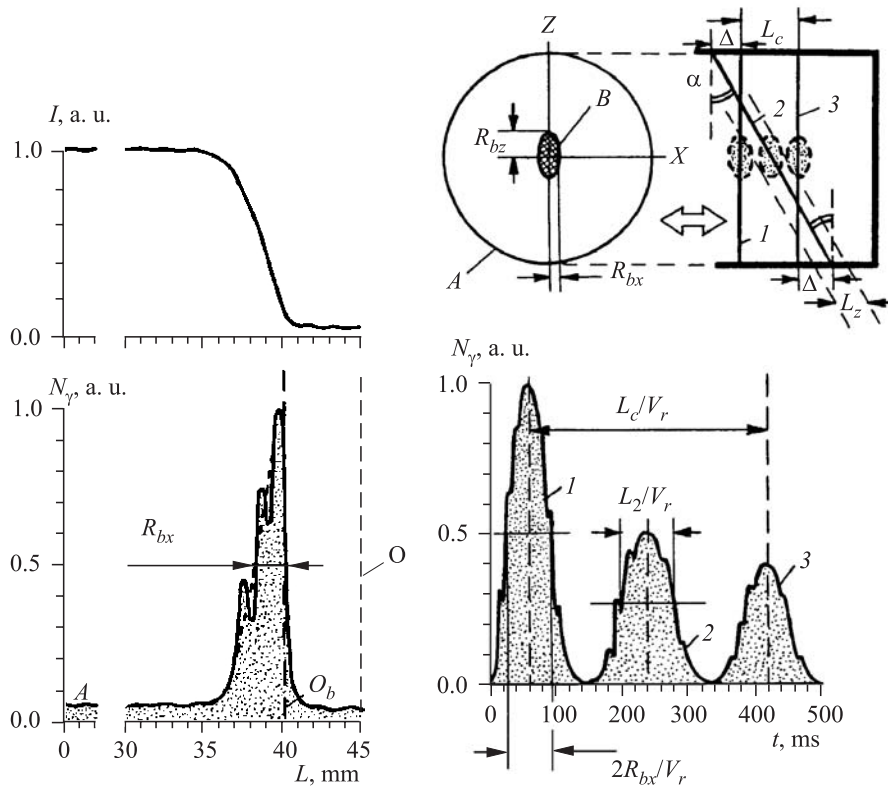


Fig. 4. Dependence of the current (I) of the circulating deuteron beam and intensity of radiation (N_γ) of a polyethylene foil of thickness $2.2 \mu\text{m}$ on the value of the target space displacement in the direction from the external radius. $E_k/A = 1.6 \text{ GeV/nucleon}$

Fig. 5. Scheme of the horizontal displacement of N-shaped internal target of the carbon fibres and dependence of the intensity of its radiation (N_γ) on time

position of the curve 2 is located in approximately the same distance (in time) from maxims in the signals from fibres 1 and 3 it indicates that the beam axis in the experimental region is very close to the plane of the symmetry ($Z = 0$) of the beam transfer line. Let us assume that the geometrical cross section of the beam has the form of canonical ellipse and that the angle α between the fibres 1, 2 and 3 as well as the measured value of R_{bx} are known, then one can determine the vertical beam size

$$R_{bz} = R_{bx} \text{ctg } \alpha \sqrt{(L_2/2R_{bx})^2 - 1}.$$

In this expression the value L_2 is equal to the space width at half-height of the distribution 2 for such target velocity when the amplitudes of the signals 1 and 3 are of the same order and their widths are approximately the same. For example, when using the target with $L_c = 20$ mm, $\alpha = 27^\circ$ and having the measured values $R_{bx} \approx 2$ mm, $L_2 \approx 5$ mm one gets $R_{bz} \approx 3$ mm. By division of the areas S_1/S_3 under the curves 1 and 3 one can estimate the average lifetime T_b of the deuteron beam interacting with it. Here with the effective thickness of thread-like target during its crossing of the beam can be estimated

$$t_g \approx \rho \cdot d^2 / 2R_{bx},$$

where d and ρ are diameter and density of the fibre matter, respectively. If we have interaction time as indicated in Fig. 5 and $S_1/S_3 \approx 1,5$ the obtained value of $T_b \approx 1$ s is in good match with the theoretical value of the product $T_b \cdot t_g$, which is calculated by employing the algorithm presented in [23] for deuteron energy of 1.6 GeV/nucleon. If we assume Gaussian distribution of the particles in transverse phase space ($R_{bi}/\sigma_{bi} = 1,18$; $\eta \cdot \sigma_{bi} = \sqrt{\beta_i \cdot \epsilon_i(\eta)}$; $i = x, z$), then for the measured values of R_{bi} and calculated values of β_i functions of the accelerator at the internal target region [30], we have obtained the following estimations of emittance of the circulating deuteron beam with energy of 1.6 GeV/nucleon: $\epsilon_x(\eta = 3) \approx 3$ mm·mrad, $\epsilon_z(\eta = 3) \approx 7$ mm·mrad.

From the point of view of minimization of particle losses and optimization of working mode of the accelerator the scanning of the beam by means of the internal target at the stages of injection and acceleration represents an independent task. In this case using the light radiation technique one can control in operative way the evolution of the beam space characteristics both in static positions of the target in various regions of the beam transfer line and during its radial motion along the definite space-time trajectory. These potentialities are demonstrated by results presented below. They were obtained during the investigation of the beam Nuclotron dynamics when running in the working modes different from the above mentioned ones.

In experiments with the deuteron beam with intensity of $\sim 10^{10}$ /spill as scanning probes we have used the same targets as in physics experiments, i. e.: polyethylene film of thickness 12 μ m and of width 2 mm and carbon fibre of diameter 8 μ m. Both of them had the height sufficient enough to cross fully the beam transfer line. The measurements have proved that the polyethylene target had higher sensitivity. Its light was detected by photoelectron multiplier at the energy of injection ($E_{d|i} = 5$ MeV/nucleon, $H = 0.3$ kg) and at the beginning of acceleration. Placing this target at static position (relatively to the beam transfer line axis — radius R_0) before the injection and then changing its position successively in horizontal direction within the transfer line diameter 90 mm made it possible to determine (by detecting the light radiation) the position and typical

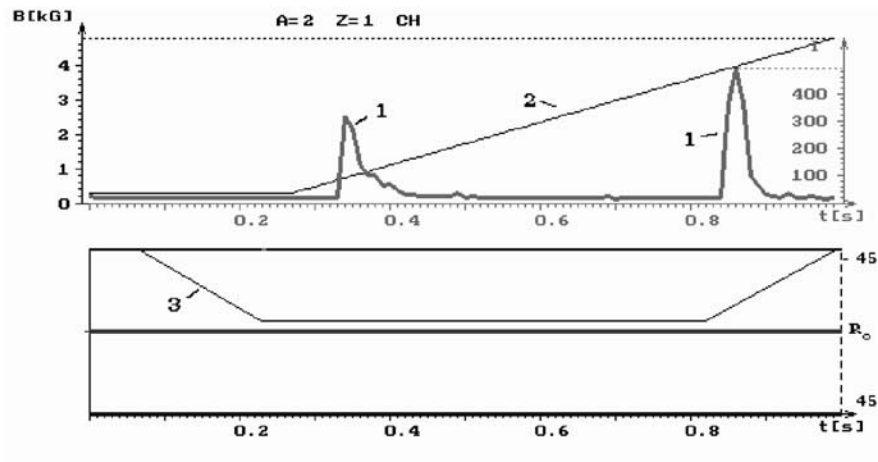


Fig. 6. Signals (1) (in relative units, to the right) of the light radiation of a scanning polyethylene target probe in its interaction with the deuteron beam at the stage of acceleration increase of the magnetic field B (2) of dipoles in real Nuclotron working mode in time (t). Below — the space-time trajectory (3) of the target in the beam transfer line of diameter 90 mm

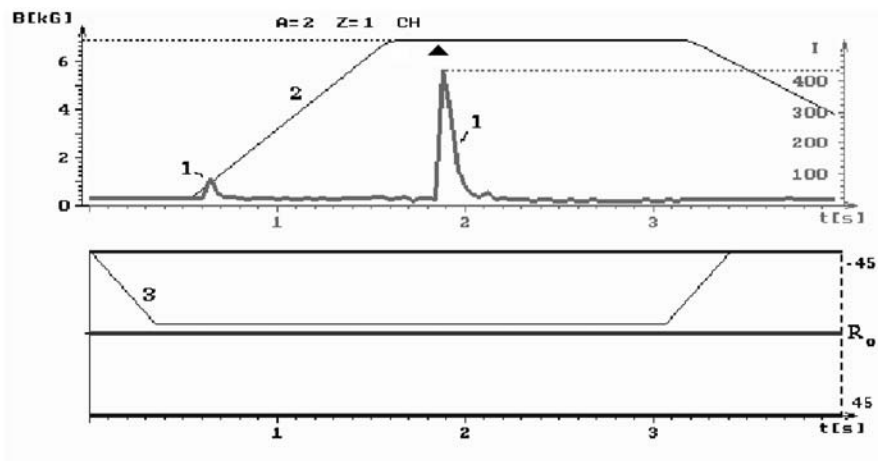


Fig. 7. The same as in Fig. 6 but with full cycle of the magnetic field. The moment when the RF-field switching off is denoted by triangular index

size of the beam. In the obtained results for $H = 0.3$ kg one can observe a wide flat plateau of almost identical interaction intensities in the range $(R_0 - 5 \text{ mm}) \div (R_0 - 30 \text{ mm})$. Figures 6–9 illustrate the spatial behavior of the beam for

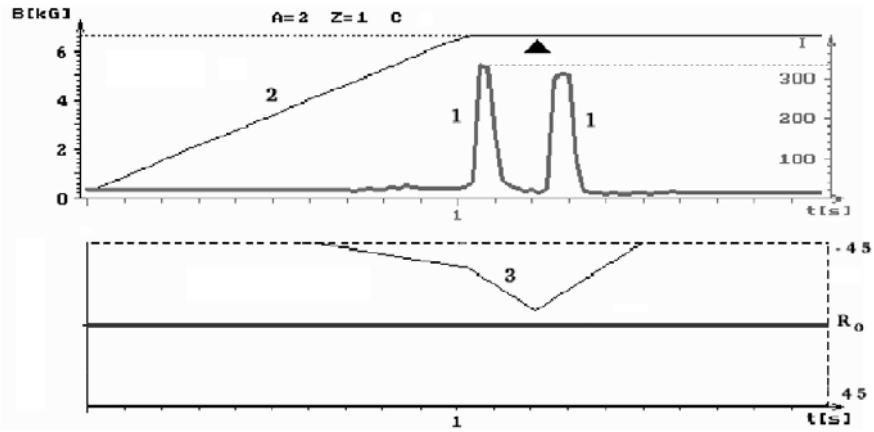


Fig. 8. Signals of the light radiation of a scanning carbon target of diameter $8 \mu\text{m}$ in its interaction with a deuteron beam energy of 1.6 GeV/nucleon. The notations have the same meaning as in Fig. 6. The moment when the RF-field is switched is denoted by triangular index

the given Nuclotron working mode. In the upper part of the figures we present the time dependence of both the magnetic field of the dipoles of the accelerator

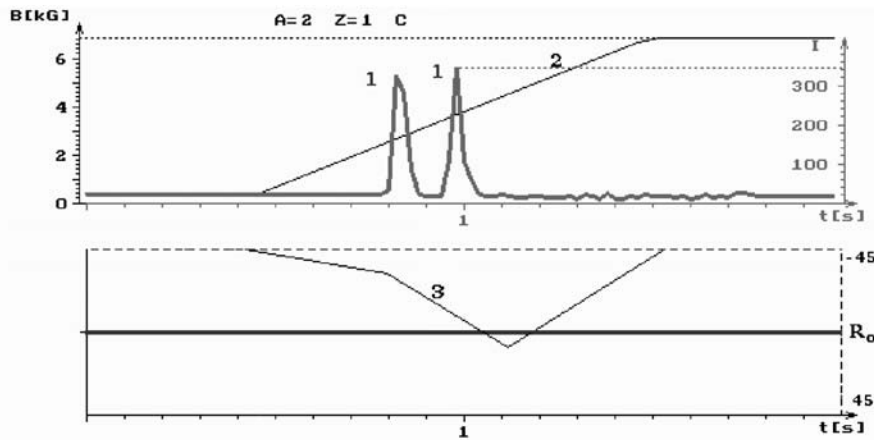


Fig. 9. The same as in Fig. 6 but with the scanning carbon target of diameter $8 \mu\text{m}$ and different space-time trajectory

and signals from the light radiation of the internal target, respectively. In the lower part of the figures we present the space-time trajectory of the target motion in the range of real cross size of the beam transfer line. Taking into account the above mentioned beginning beam position, the motion of the target started from the inside radius ($R < R_0$). Figure 6 illustrates the situation at the beginning stage of the acceleration. First during the forward motion the polyethylene target interacts only with the beam halo. Later on the back way it interacts entirely with the whole beam of higher energy and significantly smaller sizes. Figure 7 demonstrates the character of the beam interaction when the target is positioned statically in the space. Except halo-interaction at the beginning of acceleration the radiation is absent in the whole range of the existing RF-field. Only at the moment of switching it off when the magnetic field reaches the «plateau» the accelerated beam is shifted in the direction to R_0 and interacts again with the polyethylene target. This space shift of the accelerated beam with slightly changed trajectory of the target motion is illustrated in Fig. 8. The first signal coming from carbon fibre radiation and measured at the moment of switching on the RF-field has an average position of $\bar{R} = R_0 - 25$ mm. The second signal (at the moment of switching off the RF-field) obtained already from a much broader beam corresponds to the position $\bar{R} = R_0 - 19$ mm. The dynamics of the working mode with significant displacement of the beam orbit and the increase of \bar{R} during the acceleration is illustrated in Fig. 9. The first interaction takes place when the carbon fibre crosses the beam and goes in the direction to higher R . However, in the process of acceleration the beam is gradually shifted to the position when it overtakes the target and consequently the secondary interaction takes place.

CONCLUSION

The results presented in the paper proved that even in the region of minimum energy losses of the circulating beam the internal targets that are being used in physics experiments at the Nuclotron provide sufficient intensity of the radiation. The light radiation from targets can be utilized for the optimization of the beam-target interaction as well as for the operative control of its intensity in relative units for every accelerator cycle. It should be noted that in principle by means of this radiation one could realize also the operative control of the luminosity during the experiments. For this purpose, however, after every specified number of accelerator runs, it is necessary to calibrate integral flow of the detected photons to the number of secondary particles occurring during the same time interval with well-known cross section. Here one can utilize, e.g. the processes of elastic or quasi-elastic interactions of protons or nuclei as well as some channels of cumulative generation of the particles or the results of activation analysis of series of targets at the reactions $^{12}\text{C}(p, pn)^{11}\text{C}$, $^{\text{nat}}\text{Cu}(p, x)^{24}\text{Na}$, $^{27}\text{Al}(p, 3pn)^{24}\text{Na}$, etc.

The above-presented data of transverse sizes (R_{bx} , R_{bz}) and space position of the circulated beam with constant energy are not the result of dedicated systematic measurements of the beam space characteristics by means of internal targets. These data were obtained during the process of the choice of the optimal space-time trajectory as well as during the event data acquisition while carrying out experiments in relativistic nuclear physics. However, the demonstrated potentialities indicate the expedience of their use during the adjustment and tuning of the working mode of the accelerator for particular experiments as well as in the control of the beam characteristics during the experiment itself. The same applies to the presented results from experiments using the targets as scanning probes at the stage of injection and acceleration. For the scanning purposes, as well as for experimental purposes, we have used the same internal targets in one Nuclotron run.

Acknowledgements. The authors would like to express their gratitude to colleagues from SPHERE collaboration and accelerator departments of the Veksler and Baldin Laboratory of High Energies for their help in carrying out the investigations.

REFERENCES

1. *Novikov V. P., Serga E. V., Kharlamov A. V.* // Proc. of the 2nd Eur. Part. Accel. Conf. Nice, 12–16 June 1990. V. 1. P. 765.
2. *Albert A. et al.* // Nucl. Instr. and Meth. A. 1992. V. 317, No. 1–2. P. 397.
3. *Bosser J., Mann J., Ferioli G., Wartski L.* // Nucl. Instr. and Meth. A. 1985. V. 238, No. 1. P. 45.
4. *Borovkov S. D. et al.* // Nucl. Instr. and Meth. A. 1990. V. 294, No. 1. P. 101.
5. *Pollak R. E., Klassen M., Lash J., Sloan T.* // Nucl. Instr. and Meth. A. 1993. V. 330, No. 1–2. P. 27.
6. *Tron A. M.* 14-e Soveschanie po uskoritelyam zaryazennyh chastits (sbornik dokladov), Protvino, 1994. V. 2. P. 85.
7. *Burtin G. et al.* // Proc. of the Eur. Part. Accel. Conf. 2000. V. 1. P. 256.
8. *Avdeichikov V. V.* // Yadernaya fizika. 1989. V. 50. P. 409.
9. Proc. of RIKEN BNL Research Center Workshop. V. 7. «RHIC Spin Physics», April 27–29, 1998. BNL-65615. P. 151–202.
10. *Anisimov Yu. S., Artiomov A. S., Arhipov V. V., Afanasiev S. V. et al.* // Particles and Nuclei, Letters. 2004. V. 1, No. 1[118]. P. 68.
11. *Asseev A. A., Sokolov S. V.* // Proc. of the 2nd Eur. Part. Accel. Conf. Nice, 12–16 June 1990. V. 2. P. 1725.
12. Proc. of the 4th Workshop on the Medium Energy Electron Cooling (MEEC'98, Dubna). Dubna, 1999.
13. *Asseev A. A., Myae E. A., Sokolov S. V., Fedotov Yu. S.* // Nucl. Instr. and Meth. A. 1992. V. 324, No. 1–2. P. 31.

14. *Tsyganov E., Taratin A.* // Nucl. Instr. and Meth. A. 1995. V. 363, No. 3. P. 511.
15. *Ado Yu. M.* Trudy desyatogo Vsesoyuznogo soveschaniya po uskoritelyan zaryazennyh chastits (Dubna, 21–23 oktyabrya 1986 g.), Dubna, 1987. V. 2. P. 346.
16. *Amaldi U. et al.* // Phys. Lett. B. 1971. V. 36. P. 504; Proc. of the 16th Int. Conf. on High Energy Physics (Batavia, 6–13 September), 1972. P. 954.
17. *Alfred Muller* // Nucl. Instr. and Meth. A. 1989. V. 363, No. 3. P. 511.
18. *Shafranov M. G.* // ECHAYA. 1974. V. 5, No. 3. P. 645.
19. *Ekström C.* // Nucl. Instr. and Meth. A. 1995. V. 362, No. 1. P. 1.
20. *Agapov N. N., Kovalenko A. D., Malakhov A. I.* // Atomnaya energiya. 2002. V. 93, No. 6. P. 479.
21. *Baldin A. M., Malakhov A. I.* // Nucl. Phys. A. 1994. V. 566. P. 611c.
22. *Artiomov A. S. et al.* // JINR Rapid Communications. 1996. No. 1[75]. P. 95.
23. *Artiomov A. S.* // Nucl. Instr. and Meth. A. 1995. V. 366, Nos. 2–3. P. 254.
24. *Artiomov A. S., D'yachenko V. M., Kovalenko A. D.* JINR Preprint P9-95-242, Dubna. 1995.
25. *Malakhov A. I. et al.* // Nucl. Instr. and Meth. A. 2000. V. 440. P. 320.
26. *Malakhov A. I.* // Proc. of the Intern. Workshop «Relativistic Nuclear Physics: From hundreds MeV to TeV» September 30 – October 5, 1996, Cozopol. Dubna, 1997. V. 1. P. 11.
27. *Anisimov Yu. S., Atanasov I., Afanasiev S. V. et al.* // JINR Rapid Communications. 1998, No. 5[91], P. 25.
28. *Slepnev L. V., Baldin A. A., Slepnev V. M.* // Proc. of the Int. Workshop «Relativistic Nuclear Physics: From hundreds MeV to TeV» June 26 – July 1, 2000, Stara Lesna, Slovak Republic. Dubna, 2001. P. 308.
29. *Artiomov A. S., Kliman Ya., Morhac M., Turzo I.* JINR Communication P9-97-126. Dubna, 1997.
30. *Vasilishin B. V., Issinsky I. B., Mikhailov V. A., Tarovik M. N.* JINR Communication 9-86-512. Dubna, 1986.

Received on June 24, 2004.

Корректор *Т. Е. Попеко*

Подписано в печать 27.07.2004.

Формат 60 × 90/16. Бумага офсетная. Печать офсетная.

Усл. печ. л. 0,86. Уч.-изд. л. 0,9. Тираж 190 экз. Заказ № 54542.

Издательский отдел Объединенного института ядерных исследований
141980, г. Дубна, Московская обл., ул. Жолио-Кюри, 6.

E-mail: publish@pds.jinr.ru

www.jinr.ru/publish/